

A survey for low luminosity quasars at redshift $z \sim 5$

Sharp R.G.^{1,*†}, Crampton D.^{2†}, Hook I.M.³ and McMahon R.G.^{1†}.

¹*Institute of Astronomy, Madingley Road, Cambridge, CB3 0HA, UK*

²*Dominion Astrophysical Observatory, HIA, National Research Council of Canada, Victoria, B.C. V9E 2E7, Canada*

³*Department of Physics, University of Oxford, Nuclear & Astrophysics Laboratory, Keble Road, Oxford, Ox1 3RH, UK*

e-mail: rgs@ast.cam.ac.uk

15 December 2018

ABSTRACT

We present the results of a multi-colour (*VIZ*) survey for low luminosity ($M_B < -23.5$) quasars with $z \sim 5$ using the 12K CCD mosaic camera on CFHT. The survey covers 1.8deg^2 to a limiting magnitude of $m_z = 22.5$ (Vega), about two magnitudes fainter than the SDSS quasar survey. 20 candidates were selected by their *VIZ* colours and spectra for 15 of these were obtained with GMOS on the Gemini North telescope. A single quasar with $z = 4.99$ was recovered, the remaining candidates are all M stars.

The detection of only a single quasar in the redshift range accessible to the survey ($4.8 < z < 5.2$) is indicative of a possible turn over in the luminosity function at faint quasar magnitudes, and a departure from the form observed at higher luminosities (in agreement with quasar lensing observations by Richards *et al.* (2003)). However, the derived space density, of quasars more luminous than M_B (Vega) < -23.5 , of $2.96 \times 10^{-7} \text{Mpc}^{-3}$ is consistent at the 65% confidence level with extrapolation of the quasar luminosity function as derived by Fan *et al.* (2001a) at $m_i < 19.6$ (Vega).

Key words: quasars: general, galaxies: active

1 INTRODUCTION

High redshift quasars provide direct probes of conditions near the epoch of re-ionization when galaxies were first being assembled. Thus far only the most luminous members of the high redshift population of quasars have been studied, most notably with the Sloan Digital Sky Survey (SDSS York *et al.* (2000)). However, little is known about the space density of quasars at lower luminosities

At high luminosities ($M_B < -25$) Fan *et al.* (2001a) use observations from the SDSS over the redshift range $4 < z < 5$ to define a quasar luminosity function. Space density estimates based on the detections of the first quasars at $z > 5.8$ (Fan *et al.* (2003)) are incompatible with the strong evolution model proposed for the quasar luminosity function by Warren, Hewett and Osmer (1994). A primary goal of the present survey is to probe more than two magnitudes fainter than SDSS.

Two of the major uncertainties in the role of quasars in the early Universe are the transition luminosity between the observed steep bright end of the luminosity function and

the slope of the lower luminosity region of the distribution function, which is constrained to be shallower to prevent the over production of intermediate mass relic black holes at lower redshift.

Both the Big Throughput Camera 40deg^2 survey (BTC40) of Monier *et al.* (2002) and the Wide Field Survey of the Isaac Newton Telescope (INTWFS) (Sharp, McMahon, Irwin and Hodgkin (2001), Sharp (2002)) probe the high redshift ($z > 4.6$) quasar luminosity function to greater depths than that reached by SDSS. These surveys cover sufficient area to recover five quasars with $z > 4.6$ to date. Both surveys report results consistent with extrapolation of the single power law approximation to the luminosity function derived by Fan *et al.* (2001a) with little evidence for any turn over to $M_B < -25$. If such a turn over exists, and assuming a double power law form for the luminosity function (as presented by Boyle *et al.* (2000) for the 2df quasar survey at $z < 3$), then it can be shown that for a non divergent faint end slope of the luminosity function (L^β , $\beta > -2$) the major contribution of quasars to the ionising UV background at high redshifts is emitted at the knee point of the function, an analogue to the fiducial parameter of the galaxy luminosity function, L^* .

In this work we present the results of a new survey program to probe the quasar luminosity function to $M_B < -23.0$ at $z \sim 5$ with a view to constraining the faint end slope of the quasar luminosity function below L^* .

* E-mail : rgs@ast.cam.ac.uk

† Visiting Astronomer, Canada-France-Hawaii Telescope operated by the National Research Council of Canada, the Centre National de la Recherche Scientifique de France and the University of Hawaii.

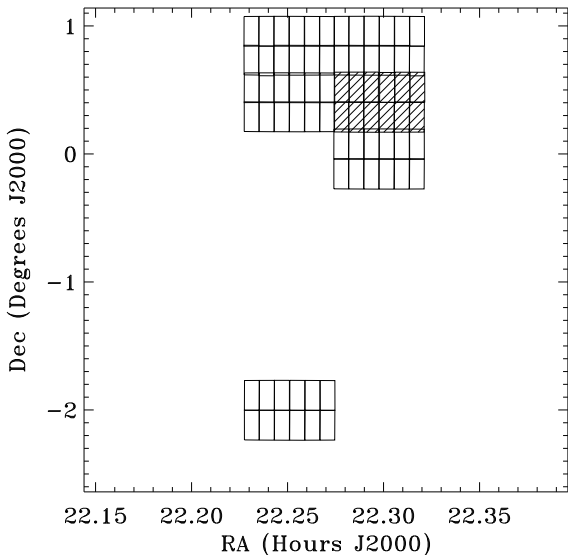


Figure 1. The location of individual CCD footprints for the 6 pointing observation of the CFDF 22hr field are shown. The total survey area, observed in VI and Z bands, is 1.77deg^2 . Observational details are given in table 1 and filter response curves are shown in Figure 2. The shaded region represents the 0.3deg^2 field with deeper observations.

Conventional Vega magnitudes are used throughout this work. Except where explicitly stated to the contrary a cosmology is adopted throughout such that $H_0=70 \text{ Km s}^{-1} \text{ Mpc}^{-1}$, and $\Omega_M=0.3$, $\Omega_\Lambda=0.7$.

2 OBSERVATIONS : OPTICAL IMAGING DATA

The imaging data were obtained with the 3.6m Canada-France-Hawaii (CFH) Telescope and the CFH12K camera. CFH12K is a close packed mosaic of 12 back side illuminated MIT Lincoln Laboratories CCDs giving a total field of view in a single observation of $42 \times 28\text{arcmin}$ and a pixel size of 0.206arcsec . The cosmetic quality of the mosaic is good with only one chip significantly affected by bad columns. Coupled with the excellent seeing routinely obtained at CFHT, the fine pixel scale allows excellent morphological classification of objects leading to a reduction of the number of marginally extended non quasar sources in the candidate list.

Observations were obtained in the VI and Z bands during the six nights 12-17 September 1999 interleaved with observations for alternate projects. Details are given in table 1. Figure 1 shows the pointing layout for the Canada-France Deep Field (CFDF: McCracken *et al.* 2001)) 2215+00 field from which the observations presented here are drawn. Anderson *et al.* (2001) subsequently identified a high luminosity $z = 4.99$ quasar within the 2215+00 field using data from SDSS. The recovery of this objects as a candidate quasar is discussed in section 4.

The data form part of an extended survey project of $\sim 6.2\text{deg}^2$ observed in the VI and Z bands. I band imaging

from the public NOAO survey¹ field at 02:07–04:30(J2000) will be used in conjunction with V and Z band imaging obtained with CFH12K. Candidate selection and spectroscopic followup observations have been carried out on a 1.8deg^2 region of the survey centred on the Canada-France Deep field region at $22:45+00:30$ (J2000) for which VI and Z data have been obtained.

Figure 2 shows the filter transmission curves for the filters used in the survey. With accurate star/galaxy separation, possible here due to the excellent seeing during the observations and the well matched pixel scale of the CFH12K camera, the dominate contaminant population within candidate lists for most high redshift quasar colour selection surveys is low mass stars. The extended red tail of the I filter is therefore not ideal for this work since the overlap between the I and Z filters reduces the power of the $I - Z$ colour index to identify low mass stars. However, the VIZ filter set, and the associated colour-colour diagram (Figure 4), does provide sufficient discrimination between quasars at redshift $z > 4.8$ and low mass stars.

2.1 Imaging data reduction

The data were processed using IRAF and the MSCRED package. Twilight flat field frames are required to facilitate the removal of interference fringes from the I and Z data. Fringe removal is carried out by iteratively scaling and subtracting a master fringe frame to minimise residual background variations. The process is automated through the use of software created as part of the Isaac Newton Telescope Wide Field Camera (INTWFC) data reduction pipeline (Irwin and Lewis (2001)). The master fringe frame is compiled on a nightly basis from flat fielded sky observations. Fringing in the Z band is present at the 7-10% level before processing. Residual fringing remains at the 1-2% level prior to image alignment and stacking. Figure 3 gives an example of the results of the data reduction procedure.

Object catalogue generation, morphological classification and the computation of an astrometric solution was performed using elements of the INTWFC pipeline (Irwin and Lewis 2001)) and with the aid of the GAIA image analysis tool². Aperture photometry is derived based on a median seeing radius aperture (0.8arcsec) and is used for VI and Z images. An aperture correction is derived on a chip-by-chip bases from a curve of growth analysis of bright, non saturated stars in the field. The World Coordinate System (WCS) is used to merge the object catalogues across the VI and Z filters with the Z catalogue used as the reference. Flux calibrations is achieved with observations of standard star fields from the Landolt (1992) catalogue (primarily L95 and L110). Observations were recorded at several locations across the CCD mosaic.

3 COLOUR SELECTION OF CANDIDATES

At $z > 3$ the optical colour indices of quasars are dominated by the unabsorbed non-thermal blue continuum longward

¹ <http://www.archive.noao.edu/ndwfs/>

² <http://star-www.dur.ac.uk/~pdrafter/gaia/gaia.html>

Table 1. Observational details.

Field	RA Dec (J2000)	Area	Observations	Depth 5 σ (Vega)†		
Canada-France Deep Field	22:17 +00:24	0.31deg ²	$V \times 4h, I \times 1h, Z \times 1h$	$m_V < 26.1$	$m_I < 24.5$	$m_Z < 23.3$
Canada-France Deep Field	22:17 +00:24	1.21deg ²	$V \times 1h, I \times 0.5h, Z \times 0.5h$	$m_V < 25.5$	$m_I < 24.0$	$m_Z < 23.1$
Anon-22	22:15 -02:00	0.31deg ²	$V \times 1h, I \times 0.5h, Z \times 0.5h$	$m_V < 25.5$	$m_I < 24.0$	$m_Z < 23.1$
NOAO Deep field	02:07 -04:30	4.25deg ²	$V \times 1h, Z \times 0.5h$	$m_V < 25.5$		$m_Z < 23.1$
NOAO Deep Wide-Field Survey	02:10 -04:30	4.25deg ²	—		$m_I < 25.5$ †	

Notes: † Depths are 5σ derived in 0.8arcsec radius (median seeing) aperture. For the 02:07–04:30 NOAO field, I band data from the public NOAO Deep Wide-Field Survey will be used to complement CFH12K V and Z band observations. The I band NOAO limit is 5 σ in 2arcsec aperture taken from <http://www.noao.edu/noao/noaodeep/>.

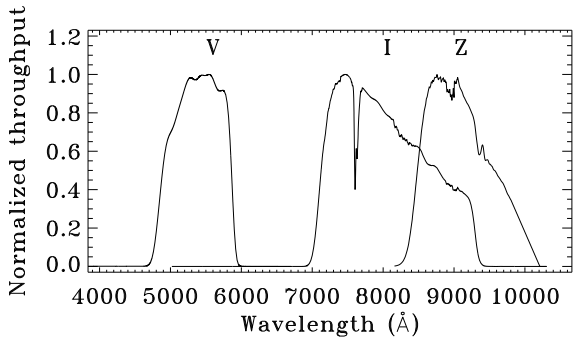


Figure 2. Filter pass bands used for the observations. Throughputs have been normalised to unity for comparison. Models of atmospheric transmission and CCD quantum efficiency have been included with the filter response functions.

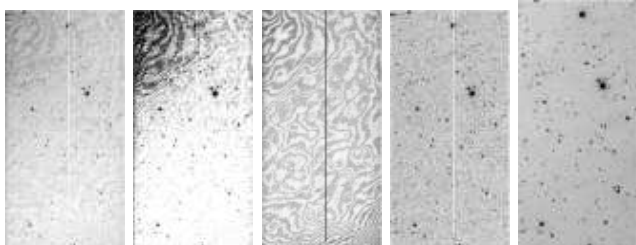


Figure 3. Example of the defringing process applied to I and Z band imaging data. A sequence of Z band frames are shown. All images are scaled to a common gray-scale level with the exception of the left-most frame which is shown with an extended scale. Images are (left to right); Flat fielded frame with fringing, frame 1 repeated with gray-scale common to remaining images, master fringe frame, defringed frame and finally the stacked frame (combining 6 \times 600sec exposures of the CFDF region).

of Ly α ($\lambda 1216\text{\AA}$) in the quasar rest frame and the effects of neutral hydrogen absorption in the Inter Galactic Medium (IGM) shortward of the Ly α emission line. At redshift $z \sim 5$ the spectral break across Ly α falls between the V and I bands.

Figure 4 shows a colour-colour diagram derived from CFH12K imaging in the VIZ bands for a 0.2deg^2 subsection of the CFDF field. The predicted quasar colour track, as a function of redshift, is over plotted. The colour track is computed assuming an underlying quasar spectrum based on a power law with spectral index $S_\nu \propto \nu^{-0.5}$ and with an emission line spectrum based on the composite spectrum of Vanden Berk *et al.* (2001). The absorption model for the

intervening Ly α forest (IGM) is taken from Madau (1995). The stellar main sequence is clearly visible as the heavily populated strip in the centre of the plot. All objects classified as stellar and with $m_Z < 22.5$ are shown.

Candidate high redshift objects are identified in the diagram as stellar objects lying below the stellar locus. To establish the selection criteria the stellar locus in the colour-colour diagram is approximated by a linear fits of the form,
$$(V - I) = m \times (I - Z) + c, \quad (1)$$

an offset from the locus is then chosen so as to minimise the stellar contamination of the candidate list while maximising the accessible redshift range. The colours selection criterion then becomes,

$$(V - I) > 0.22, (I - Z) < -0.1, \quad (2)$$

$$(V - I) = 6.06 \times (I - Z) + 0.83, (I - Z) < 0.6,$$

Once selected as a candidate quasar, candidates are visually inspected to check the validity of the photometry. This step is required to identify spurious sources such as objects in the diffraction spikes of bright stars. Two example candidates are shown in Figure 5. A finding chart is also generated based on the Z band image at a larger scale. Image defects such as stellar halos and poor fringe correction are readily identified on inspection of these charts. Such candidates are flagged as lower priority accordingly. While the image quality of the CFH12K mosaic is generally high, this step greatly reduces the number of candidates requiring spectroscopic observation. Since targets are selected as outliers in colours space, we are particularly vulnerable to objects with spurious photometry.

3.1 Stellar classification requirements

Candidate high redshift quasars are expected to appear as unresolved (PSF limited) point sources in I and Z band observations with little or no detectable flux in the V band due to absorption in the IGM.

Candidate selection based on classification as a point source in the Z band is required to reduce the target list to a practical size for observation. Clearly a V band classification cannot be used since classification becomes unreliable at the survey limit and is impossible for drop out objects. Classification based on the I band would be preferable due to the reduced residual fringing when compared to the Z band. However, a problem with the focus mechanism of the camera during observations resulted in a degradation of the image quality (a slight ellipticity) for I band observations.

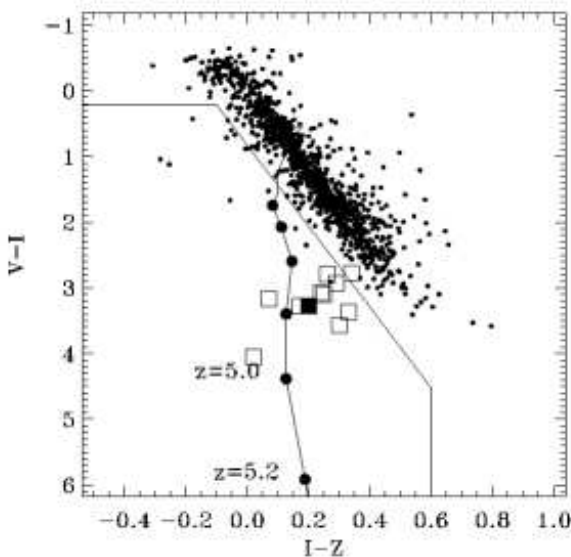


Figure 4. Candidate selection is performed based on the colour-colour diagram constructed from the VI & Z bands. The theoretical quasar locus is marked at redshifts $z=5.0$ and 5.2 (filled circles indicate lower redshifts with $\Delta z=0.2$). Open symbols mark candidate quasars drawn from the full 1.8deg^2 survey. The filled square represents the known $z=4.99$ quasar pSDSSJ2216+0013. The stellar locus is compiled from a 0.2deg^2 subsection ($\sim 10\%$) of the CFDF survey area.

Object classification is therefore based on Z band imaging with I band classification used only as a secondary indicator for assessing quasar candidates. The actual classification of an object as a point source is derived from a curve of growth analysis from object fluxes recorded in progressively larger radii apertures centred on each source (Irwin and Lewis (2001)).

The assumption of a stellar classification for quasars requires that there will be no significant contamination from the quasar host galaxy. Even at the lower redshift cutoff for VIZ colour selection ($z > 4.8$) the Z band filter samples the rest frame UV spectrum short-ward of 2000\AA and any such contamination would be negligible.

3.2 Dust extinction

Any quasar selection based on rest frame UV colour indices is subject to bias against objects suffering moderate dust extinction either along the line of sight (Fall and Pei (1993)) or intrinsic to the quasar (Sharp *et al.* (2002)). In order to draw a comparison with the luminosity function of Fan *et al.* (2001a) no attempt is made to account for possible selection effects from dust reddening in the current work.

4 PSDSSJ2216+0013, A QUASAR AT $Z=4.99$

A previously known high redshift quasar was rediscovered in the field. Quasar pSDSSJ2216+0013 at $z=4.99$ (Anderson *et al.* (2001)) is readily identified as a candidate quasar in the VIZ colour-colour diagram (Figure 4). The CFDF

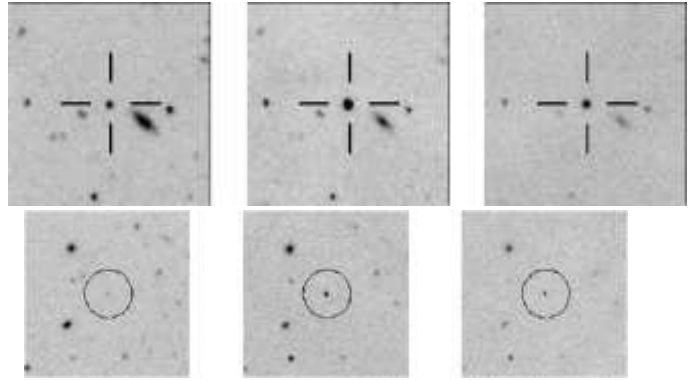


Figure 5. VI and Z band images are shown from left to right. The field size in each image is 40arcsec . Similar image sequences of all candidate quasars are examined to check the validity of photometry.

Upper : The rediscovered SDSS high redshift quasar pSDSSJ2216+0013 at $z=4.99$.

Lower : Identified as a quasar candidate by it's very red, $V - I = 3.57$, colour index, cfh12k8 (Table 3) is identified spectroscopically as an early type M star.

was not preselected for observation based on the presence of pSDSSJ2216+0013 within the field.

Figure 5 shows the VIZ images for this object. The observational details are given in table 2 and are compared with the reported observations of pSDSSJ2216+0013 from the SDSS. No new spectroscopic observations of pSDSSJ2216+0013 have been performed.

The spectrum of pSDSSJ2216+0013 is unremarkable, with the exception of the high redshift and bright magnitude. The discover spectrum (Anderson *et al.* (2001)) shows the typically strong continuum break across a strong narrow Ly α /N ν blend supporting the photometric measurements. Given these sharp features and the slight mismatch between the SDSS and CFH12K filter systems, plus potential for quasar variability, the observed magnitudes and colours are in good agreement. The coordinate offset between the reported SDSS position and that measured from CFH12K is $\sim 0.28\text{arcsec}$ (-0.2arcsec in each axis). This is at the predicted limit of the external accuracy of the survey WCS computed with the INTWFC data processing pipeline. This accuracy is primarily limited by the accuracy with which unsaturated objects within the imaging data can be tied to a well defined WCS from astrometric survey data. Internally to the survey the astrometric accuracy between different filter observations is at the $\sim 0.1\text{arcsec}$ level.

5 OBSERVATIONS : SPECTROSCOPIC

Observations of fifteen quasar candidates were obtained with the GMOS spectrograph (Murowinski *et al.* (2003) in preparation, Hook *et al.* (2003) submitted) during regular queue-scheduled observations on the Gemini North telescope in November 2001 and June-July 2002. The November observations were among the first regular science observations with GMOS North and, as a result, could not be taken with the proper blocking filter to remove the second order spectra. Conditions were photometric or near-photometric for the majority of the observations and the image quality was

Table 2. The rediscovered SDSS high redshift quasar pSDSSJ2216+0013.

Name	pSDSSJ2216+0013	
Redshift	4.99	
M_B	-26.6	
SDSS	$\sinh AB$	Vega
r	21.78	21.60
i	20.30	19.88
z	20.33	19.77
i-z	-0.03	0.11
Ra Dec (J2000)	22:16:44.02	+00:13:48.3
CFH12K		Vega
V	—	23.01
I	—	19.73
Z	—	19.56
V-I	—	3.28
I-Z	—	0.20
Ra Dec (J2000)	22:16:44.034	+00:13:48.51

better than 1 arcsec. A 0.75'' slit was used with the R400 grating and the detector was binned 2×2 , yielding a dispersion of 1.4 Å/pixel and a spectral resolution (determined by the slit width) of 9Å. The useful spectral range was typically 5900-9500Å. An OG515 filter was used to remove the second order for the 2002 observations. A single exposure was obtained for most objects, with exposure times ranging from 1800s to 2400s (for the faintest targets).

The data were reduced following standard methods with the Gemini IRAF tools³ to pre-process and mosaic the spectra from the 3 CCD detectors together, followed by extraction and reduction of the 1D spectra with IRAF SPECRED. An approximate flux calibration was determined from observations of standard stars with identical instrument parameters during the same period of observation (contamination from second order blue light further reduced the accuracy of the flux calibration for the 2001 November observations).

5.1 Observed spectra of candidate quasars

Details of the fifteen candidate quasars are given in table 3. No strong emission line objects are detected. Indeed, all of the observed spectra show strong similarities and are suggestive of early type M stars. In order to determine the classification of stars prone to selection using the *VIZ* colour diagram a composite stellar spectrum is constructed by co-adding the individual observations of each candidate (Figure 6).

The composite spectrum is examined following the classification schemes of Kirkpatrick, Henry and McCarthy (1991) (for K-M stars) and Kirkpatrick *et al.* (1999) (for later type L stars). The presence of pronounced absorption features, coincident with the expected location of TiO bands, suggest identification with stars later than \sim M2. The lack of a broad potassium feature at \sim 7700Å is taken as evidence that the spectra are not from L stars. Absorption in VO bands becomes increasingly pronounced in later M stars. We

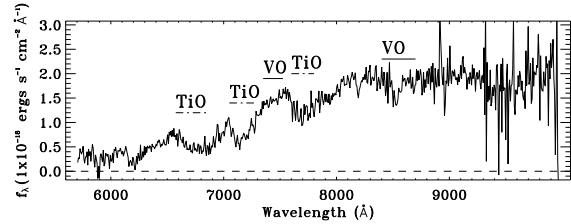


Figure 6. To provide a preliminary classification, a simple summation is performed of all the candidate spectra. The resulting spectrum is then smoothed and re-binned by a factor of five (corresponding to the spectroscopic resolution element). Following the classification scheme of Kirkpatrick, Henry and McCarthy (1991) the composite spectrum suggests, as expected from synthetic *VIZ* band photometry models, the stellar interlopers fall in the range of spectral types M2-M5. TiO absorption bands and the absence of a strong absorption features due to K suggest classification as an M star. The weakness of VO absorption at longer wavelengths argues against late type M stars.

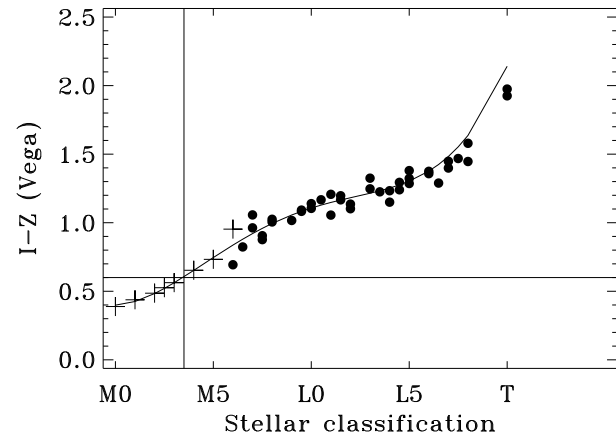


Figure 7. The colour of low mass stars as a function of classification can be computed using an atlas of stellar spectra. The $I - Z$ colours, in the CFH12K filter system, are in agreement with those found by Dobbie *et al.* (2002). The colours are estimated using the Keck LRIS spectra of Reid *et al.* (2001, <http://dept.physics.upenn.edu/~inr/ultracool.html>) for stars later than M5 and atlas of Pickles (1998, <http://archive.ast.cam.ac.uk/viz-bin/VizieR>) for M0V-M6V. Based on synthetic photometry measurements, the sample $I - Z < 0.6$ colour cut selects against stars later than M3.5.

therefore identify the composite spectra with a classification earlier than M5.

Examination of the spectra of each target individually supports the classification range (M2-5) assigned to the composite spectra. TiO absorption bands are readily identified. While the VO feature is in a region of the spectrum affected by strong OH sky residuals, there is little evidence for significant absorption.

A classification for stellar interlopers in the range M2-M5 is consistent with the synthetic photometry prediction shown in Figures 7 and those of Dobbie, Pinfield, Jameson and Hodgkin (2002).

³ <http://www.gemini.edu/sciops/instruments/gmos/gmosIndex.html>

Table 3. Details of the fifteen candidate spectroscopically observed. The primary target list contains twenty such targets, suggesting a 75% follow up completeness.

Object	RA Dec (J2000)	Magnitude (Vega)			Colour (Vega)	
		V	I	Z	V-I	I-Z
cfh12k1	22:15:55.38, +00:58:25.4	25.01	22.23	21.89	2.78	0.34
cfh12k2	22:18:30.50, +00:59:59.3	25.39	22.28	22.03	3.10	0.25
cfh12k3	22:18:06.14, +00:42:11.2	25.05	22.13	21.90	2.92	0.23
cfh12k4	22:18:33.37, +00:39:23.7	>25.36	22.57	22.31	>2.79	0.26
cfh12k5	22:18:36.88, +00:39:30.7	>25.37	22.44	22.15	>2.93	0.29
cfh12k6	22:17:39.05, +00:33:45.3	26.32	22.34	21.90	3.98	0.44
cfh12k7	22:16:28.76, +00:10:57.0	25.24	21.97	21.80	3.26	0.17
cfh12k8	22:17:29.54, +00:11:46.5	25.48	21.91	21.60	3.57	0.34
cfh12k9	22:17:47.34, +00:15:05.1	26.17	23.00	22.93	3.17	0.07
cfh12k10	22:18:40.03, +00:11:55.1	24.73	21.91	21.80	2.82	0.11
cfh12k11	22:13:40.93, -01:49:06.6	25.23	22.63	22.57	2.60	0.06
cfh12k12	22:15:42.26, -02:12:58.3	25.49	22.69	22.49	>2.80	0.20
cfh12k13	22:18:30.16, +00:09:16.9	25.56	22.20	21.87	3.37	0.33
cfh12k14	22:16:49.87, -00:13:44.0	25.49	22.85	22.74	>2.64	0.11
cfh12k15	22:16:53.65, -00:13:33.3	25.23	22.15	21.91	3.07	0.24

6 QUASAR SPACE DENSITY

A tentative quasar space density of $2.96 \times 10^{-7} \text{ Mpc}^{-3}$ (65% confidence limits $\pm 1.6 \times 10^{-6}$) is inferred for the redshift range $4.8 < z < 5.2$ and absolute magnitude, $M_B < -23.5$ (Vega) limit accessible to the 1.8deg^2 CFH12K *VIZ* survey.

The survey area is estimated via monte-carlo integration. The survey completeness function is estimated in the manner adopted by Sharp *et al.* (2001). A grid of model quasar spectra is generated, over the accessible redshift range, with parameters for the quasar spectral model, discussed in section 3, drawn at random from the distribution functions

$$\begin{aligned} \alpha &= N(-0.5, 0.3^2), \\ EW(\text{Ly}\alpha) &= N(92.91, 34.0^2) \end{aligned} \quad (3)$$

Synthetic photometry estimates are computed for each model quasar and colours are determined within the survey filter system. Representative survey photometric errors are then added to the photometry, scaling each spectrum over the magnitude range, m_z , available. The fraction of quasars recovered by the survey colour selection criteria, as a function of redshift and magnitude m_z , is recorded as an estimate of the survey completeness function.

To $m_z < 22.5$ and in the redshift range $4.8 < z < 5.2$ the survey is predicted to be 70% complete.

6.1 Improved selection criteria

The plethora of early M star interlopers in candidate lists has dogged quasar surveys at $z > 4$. Fundamentally, the spectral energy distribution of early type M stars leads to colour indices which mimics those of quasars in the redshift range $4.8 < z < 5.8$.

When the spectroscopic stage of the survey is extended to include the 4.25deg^2 NOAO field, the spectroscopic observations, reported in section 5, and the predicted colours for low mass stars (Figure 7) argue in favour of tighter colour constraints than are reported in section 3. This would re-

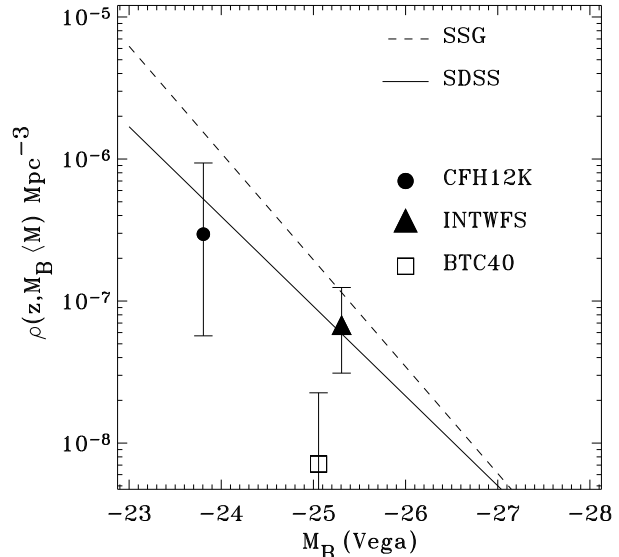


Figure 8. The quasar space density, inferred from three contemporary low luminosity high redshift surveys, is shown ($4.8 < z < 5.2$; CFH12K-this work, INTWFS-Sharp *et al.* (2001), Sharp (2002), BTC40-Monier *et al.* (2002)). Predictions from two popular forms of the luminosity function are also shown, estimated as a function of limiting absolute magnitude, M_B (Vega), and evaluated at redshifts $z = 5$ (SSG-Schmidt, Schneider and Gunn (1995), SDSS-Fan *et al.* (2001a)). Error bars indicate the 65% confidence intervals for each survey data set assuming Poisson statistics. Survey completeness corrections are applied to the CFH12K and INTWFS data points. Survey limiting magnitudes correspond to CFH12K $m_z = 22.5$, INTWFS $m_z = 21.0$, BTC40 $m_i = 21.5$.

duce the number of low mass early M stars included in the candidate list at the expense of survey completeness.

In principle, extending the wavelength baseline of the colour selection criteria allows a greater degree of separation between the two source populations. Fan *et al.* (2001b) perform targeted IR observations of *i* band drop out ob-

jects from SDSS (with repeated z photometry to confirm the validity of the single optical band photometry) to detect the first quasar at $z > 6.0$. At such high redshifts the stellar contaminants are L and T dwarfs with intrinsically redder $I - Z$ and $Z - J$ colour indices than M stars. At the lower redshifts probed by our CFH12K survey $4.8 < z < 5.2$ the $z - J \sim 0.5$ colour index of quasars is close to that of the early M star contaminant ($0.7 < z - J < 1.3$ for M0V-M5V, Figure 7). With such a colour separation between the two source populations, high accuracy photometry, often difficult to maintain over wide fields of view at low luminosities, will be required if the IR colour index is to be used in selection criteria.

Nevertheless, with the advent of large format IR mosaic cameras at 4meter class telescope facilities such as WIRCam at CFHT, WFCAM on UKIRT (with the UKIDSS Large Area Survey (LAS) of particular relevance⁴) and the VISTA survey projects it will soon be possible routinely acquire wide field IR photometry of sufficient depth and accuracy to introduce an additional colour index to reduce the contamination by low mass stars.

7 CONCLUSIONS

In conclusion, we detect only a single high redshift, $4.8 < z < 5.2$, quasar in the 1.8deg^2 of the CFH12K survey currently investigated spectroscopically. The inferred space density of $2.96 \times 10^{-7} \text{ Mpc}^{-3}$ (65% confidence limits $\pm 1.6 \times 10^{-6}$ to $\pm 7.5 \times 10^{-9}$) is lower than that predicted by the extrapolation of the Fan *et al.* (2001a) quasar luminosity function (derived for $m_i < 19.6$ (Vega)) to fainter magnitudes.

The dearth of high redshift quasars in our 1.8deg^2 survey area and the quasar density reported by Sharp *et al.* (2001), found to be in agreement with the luminosity of Fan *et al.* (2001a), is indicative of a possible turn over in the luminosity function at faint quasar magnitudes, although the detection of only a single redshift $4.8 < z < 5.2$ quasar is consistent with the luminosity function at the 65% confidence level. Further evideance for such a turnover is provided by Richards *et al.* (2003). Richards *et al.* use the apparant lack of multiply imaged quasars amongst a sample of four $z > 5.7$ quasars, identified within SDSS, to constrain the bright end slope and break point, M_B^* , of the luminosity function. Their analysis suggest a break point at $M_B^* = -24.38$ (Vega) ($M_{1450}^* = -24.0$ AB). When I band data from the public NOAO survey become available, it will be possible to triple the areal coverage of our CFH12K quasar survey.

It is worthy of note that all candidate objects have been identified with intrinsically unresolved (PSF limited) stellar sources. Both the INTWFS (Sharp *et al.* (2001)) and to a lesser degree the BTC40 (Monier *et al.* (2002)) quasar survey programs suffered from contamination of the candidate list by compact galaxies. As quasar surveys reach fainter limiting magnitudes, one progresses further down the galaxy luminosity function and the number of compact foreground galaxies becomes large. The large volume of colour space occupied by normal galaxies, which are not tied to a well

defined colour space locus as is the case with stars, means spectroscopic follow up of targets can become prohibitively expensive unless a reliable star/galaxy classification can be adopted. The high spatial resolution and excellent image quality of the CFH12K imaging system has resulted in the removal of such extended sources from our candidate lists.

ACKNOWLEDGEMENTS

RGS acknowledges the receipt of a PPARC studentship. Thanks are due to Mike Irwin, for help and guidance during mosaic data reduction and the construction of a world coordinate system, and Simon Hodgkin for useful discussions regarding the spectral features of low mass stars.

Spectroscopic observations where obtained at the Gemini Observatory, which is operated by the Association of Universities for Research in Astronomy, Inc., under a co-operative agreement with the NSF on behalf of the Gemini partnership: the National Science Foundation (United States), the Particle Physics and Astronomy Research Council (United Kingdom), the National Research Council (Canada), CONICYT (Chile), the Australian Research Council (Australia), CNPq (Brazil) and CONICET (Argentina)

REFERENCES

Anderson S.F., Fan X., Gordon T., Richards G.T., Donald P., Schneider D.P., Michael A., Strauss M.A., Vanden Berk D.E., James E., Gunn J.E. *et al.* 2001 AJ 122 503
 Boyle B.J., Shanks T., Croom S.M., Smith R.J., Miller L., Loaring N., Heymans C 2000 MNRAS 317 1014
 Dobbie P.D., Pinfield D.J., Jameson R.F. and Hodgkin S.T. 2002 MNRAS 335 79
 Fall S.M. and Pei Y.C. 1993 ApJ 402 479
 Fan X. *et al.* 2001a AJ 121 54
 Fan X. *et al.* 2001b AJ 122 2833
 Fan X. *et al.* 2003 ApJ 125 1649
 D.W. Hogg 1999 astro-ph/9905116
 Hook I.M *et al.* in prep
 Irwin M.J. , Lewis J.R. 2001 New Astronomy Reviews 45 105
 Kirkpatrick J.D., Henry T.J and McCarthy D.W.Jr 1991 ApJS 77 417
 Kirkpatrick *et al.* 1999 ApJ 519 802
 Landolt A.U. 1992 AJ 104 340
 Lupton R.H. Gunn J.E. Szalay A.S. 1999 1999 AJ 118 1406
 Madau P. 1995 ApJ, 441, 18
 McCracken, H.J., *et al.* 2001, A&A, 376, 756
 Monier E.M., Kennefick J.D., Hall P.B., Osmer P.S., Smith M.G., Dalton G.B., Green R.F. 2002 AJ 124 2971
 Murowinski R.G. *et al.* 2003 SPIE 4841 1189
 Pickles A.J. 1998 PASP 110 863
 Reid I.N., Burgasser A.J., Cruz K.L., Kirkpatrick J.D. and Gizis J.E. 2001 AJ 121 1710
 Richards G.T. *et al.* 2003 astro-ph/0309274
 Schmidt M. Schneider D.P. Gunn J.E. 1995 AJ 110 68
 Sharp R.G., McMahon R.G., Irwin M.J., Hodgkin S.T. 2001 MNRAS 326L 45

⁴ <http://www.ukidss.org/>

8 *Sharp R.G., Crampton D., Hook I.M. and McMahon R.G.*

Sharp R.G., Sabbe C.N., Vivas A.K., Oemler A., McMahon R.G., Hodgkin S.T. Coppi P.S. 2002 MNRAS 337 1153

Sharp R.G. 2002 PhD Thesis, University of Cambridge, UK
York *et al.* 2000 AJ 120 1579

Vanden Berk, D.E. et al. 2001 AJ 122 549

Warren S., Hewett P., Osmer P. 1994 ApJ 427 412

Warren S., Hewett P. 2002 2002 nec conf 369